

Screened hydrodynamic interaction in a narrow channel

Bianxiao Cui, Haim Diamant, and Binhua Lin*

The James Franck Institute, Department of Chemistry,
and CARS, The University of Chicago, Chicago, Illinois 60637

(Dated: November 5, 2018)

We study experimentally and theoretically the hydrodynamic coupling between Brownian colloidal particles diffusing along a linear channel. The quasi-one-dimensional confinement, unlike other constrained geometries, leads to a sharply screened interaction. Consequently, particles move in concert only when their mutual distance is smaller than the channel width, and two-body interactions remain dominant up to high particle densities. The coupling in a cylindrical channel is predicted to reverse sign at a certain distance, yet this unusual effect is too small to be currently detectable.

PACS numbers: 83.50.Ha, 83.80.Hj, 82.70.Dd

Diffusion along narrow channels is encountered in various circumstances, such as transport in porous materials [1] and penetration through biological ion channels [2]. Much attention has been devoted to the correlated motion in so-called *single-file* systems due to the inability of particles to bypass one another, leading to anomalous diffusion [1, 3]. The anomalous regime, however, sets in only at long enough times when particle collisions become appreciable [4]. Yet, if the channel is filled with liquid, the motion of otherwise non-interacting Brownian particles can become correlated at times shorter than the collision time through the flow field that they create. Indeed, when we observed the diffusion of micron-size colloidal particles in a water-filled channel (Fig. 1), the most striking feature was the occasional concerted motion of several close-by particles in a dynamical “train” lasting for a few seconds. In the current Letter we present a quantitative study of this coupling.

When a particle moves through a fluid it creates a flow that affects the velocities of other particles in its vicinity. Recently there has been renewed interest in such hydrodynamic interactions, particularly in confined geometries, due to their role in the behavior of colloidal suspensions and the development of techniques using digital video microscopy [5, 6, 7, 8, 9, 10]. Colloidal particles in a finite container [5], near a single wall [6, 7, 8], and between two walls [6, 9] were studied. The hydrodynamic interactions in those geometries are always attractive (i.e., creating positive velocity correlations) and long-ranged: in an unbounded fluid the interaction decays with inter-particle distance x as $1/x$ [11]; the one between particles moving near and parallel to a single wall decays as $1/x^3$ [7, 12]; and for particles moving between and parallel to two walls it decays as $1/x^2$ [13]. More constrained geometries—perpendicular to the walls in a two-wall configuration [13] and along a cylindrical tube [14, 15]—are essentially different, in that point disturbances should create flows with an exponential spatial decay. Here we demonstrate that confinement in a linear channel indeed sharply screens the hydrodynamic interaction and may even change its sign.

The experimental system consists of an aqueous suspension of silica colloidal spheres (density 2.2 g/cm^3) confined in long narrow grooves (see Fig. 1 and inset of Fig. 4). The grooves were printed on a polydimethylsiloxane substrate from a master pattern fabricated lithographically on a Si wafer (Stanford Nanofabrication Facility). A drop of suspension was enclosed between the polymer mold and a cover slip with a spacer ($\sim 100 \mu\text{m}$), so that the top of the groove was open to a layer of fluid. Digital video microscopy was used to extract time-dependent two-dimensional trajectories of the spheres (time resolution 0.033 s). Details of sample preparation and data analysis were described elsewhere [4, 16].

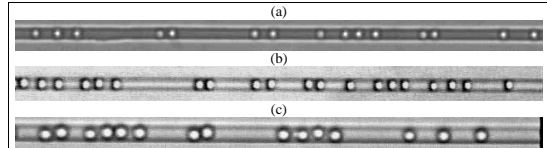


FIG. 1: Microscope images of silica colloidal spheres confined in linear grooves (cf. Table I): a) sample 1, $\eta = 0.17$; b) sample 2, $\eta = 0.35$; c) sample 3, $\eta = 0.36$.

no.	a (μm)	w (μm)	h (μm)	L (mm)
1	0.79 ± 0.02	3.0 ± 0.3	3.0 ± 0.3	2
2	1.85 ± 0.05	5.0 ± 0.1	4.0 ± 0.5	10
3	2.57 ± 0.1	7.0 ± 0.1	4.0 ± 0.5	10

TABLE I: Parameters of the three experimental samples.

We studied samples of three different parameter sets, i.e., different values of sphere radius a , channel width w , channel depth h , and channel length L ; see Table I and Fig. 1. (Spheres of sample 1 were manufactured by Duke Scientific and those of samples 2 and 3 by Bangs Laboratory.) The ratio a/w ranges between 0.26 and 0.37; it is always larger than $1/4$, such that spheres cannot bypass one another. (Higher ratios pose a difficulty in loading the spheres into the channel.) The linear packing fraction η was determined as $\eta = 2Na/l$, where l is the length of

the channel section in the field of view ($l = 106\mu\text{m}$ for sample 1 and $220\mu\text{m}$ for samples 2 and 3), and N is the number of spheres in that section.

Studies of the equilibrium structure and single-particle dynamics of sample 1 were previously reported [4, 16]. These experiments show that the colloidal motion is tightly confined to the center of the groove, with transverse fluctuations of less than $0.2a$. The particle pair-potential consists of a short-ranged (screened electrostatic) repulsion, extending to surface–surface separations of $\sim 0.2\mu\text{m}$, followed by a weak attractive well of $\sim -0.3k_{\text{B}}T$ ($k_{\text{B}}T$ being the thermal energy) at a separation of $\sim 0.3\mu\text{m}$. At the range of the dynamic coupling reported here the pair-potential is practically zero [16]. We thus neglect in the current study any transverse motion and direct interactions.

We choose to characterize the coupling by the collective and relative diffusion of particle pairs, i.e., the fluctuations of their center of mass and mutual distance. We define the collective diffusivity, D^+ , and the relative one, D^- , as

$$D^\pm(x) = \langle [\Delta x_1(t) \pm \Delta x_2(t)]^2 \rangle / 4t, \quad (1)$$

where Δx_i is the displacement of particle i during time t and x is the short-time average distance between the centers of the two spheres. The coefficients have been defined such that, in the absence of coupling, they both reduce to the self-diffusivity of a single particle, D_s . In our data analysis $D^\pm(x)$ were calculated from the histogram of short-time ($t < 0.2$ s) trajectories, i.e., the slope of the mean-square displacements, $[1/4N(x)] \sum_{i=2}^{N(x)} [\Delta x_i(t) \pm \Delta x_{i-1}(t)]^2$, as a function of t , where $N(x)$ is the number of nearest-neighbor pairs whose mutual distance x falls in the range $(x - \delta x/2, x + \delta x/2)$. (We took $\delta x = 0.22a$ for all samples.) The tracking time t must be kept sufficiently short, so that the spheres do not cross over to the anomalous subdiffusion regime [4], and their diffusion distance remains smaller than δx , so x can be assumed constant. We verified that, within experimental error, the measured slopes were constant at least in the range $t = 0.1\text{--}0.5$ s.

Figure 2 shows the measured collective and relative diffusivities for the various samples. The diffusivities sharply decay to D_s for inter-particle distances larger than about twice the channel width. Moreover, the coupling is practically insensitive to changes in density up to high values of η , implying that three-body and higher terms remain negligible. At $\eta = 0.61$ sample 1 exhibits a considerable shift of the entire curves towards lower diffusivity, i.e., a decrease in D_s [17]. These observations are in essential contrast with the case of less confined geometries, where the hydrodynamic interaction is long-ranged with significant many-body effects [5].

We now turn to a theoretical estimate of the hydrodynamic coupling. The Reynolds number of the system

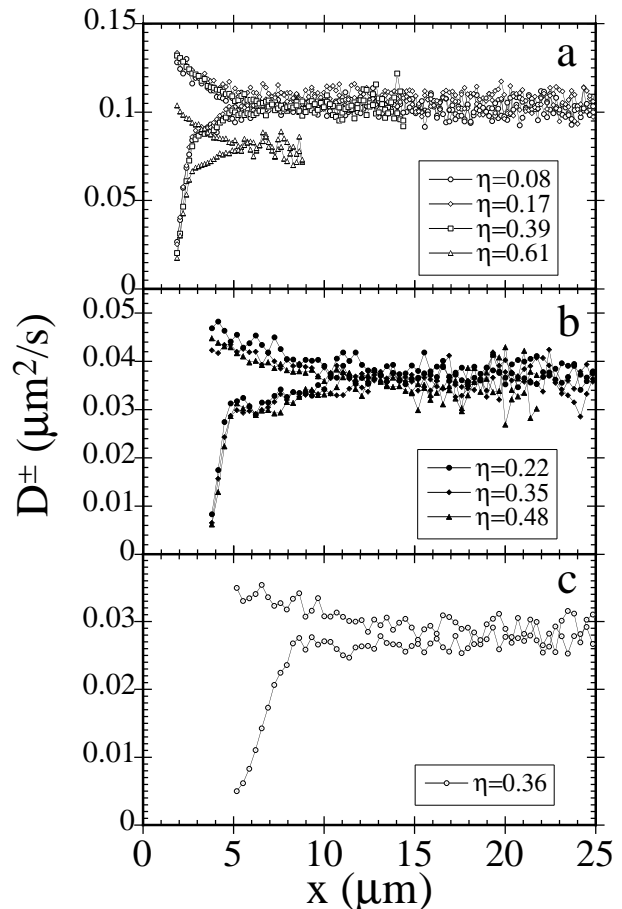


FIG. 2: Collective (D^+ , upper curves) and relative (D^- , lower curves) pair diffusivities as a function of inter-particle distance x for various values of packing fraction η . Figures a, b and c correspond to samples 1, 2 and 3, respectively.

is of order 10^{-6} . We need, in principle, to calculate the Stokes flow due to the motion of two particles, subject to no-slip boundary conditions at the surfaces of the channel and particles [11, 18]. This is technically very hard and, furthermore, we seek a description of more general applicability. We resort to three simplifications: (i) The actual geometry of a partially open, rectangular channel is replaced by an effective cylinder, of diameter $2R = \gamma w$, where γ is a geometrical prefactor of order 1, to be treated as a fitting parameter. We expect to obtain one value of γ for a square cross-section (samples 1 and 2), and another for a rectangular one (sample 3). Because of the open top of the actual channel, we also expect the effective cylinder to be significantly wider, i.e., $\gamma > 1$. (ii) The particle motion is assumed to be restricted to the central axis of the channel. (As has been noted above, this is a good approximation in our case.) (iii) The particle size is assumed to be much smaller than both the channel width, $a \ll R$, and the inter-particle distance, $a \ll x$. This requirement, though not strictly fulfilled in practice, allows us to treat the effect of one particle on

the flow near the other and near the walls as if it were exerting a point force on the fluid, i.e., to consider merely the fundamental solution (Green's function) of the Stokes flow in the channel. (This is sometimes referred to as the *stokeslet approximation* [12].)

The displacement fluctuations of a particle pair are used to define a two-particle diffusion tensor, $\langle \Delta x_i(t) \Delta x_j(t) \rangle = 2D_{ij}(x)t$, $i, j = 1, 2$, which can be decomposed into a self-diffusion term and a coupling one: $D_{ij} = \delta_{ij}D_s + (1 - \delta_{ij})D_c(x)$. The two eigenvalues, $D^\pm = D_s \pm D_c(x)$, are the collective and relative diffusivities of the pair as defined in Eq. (1). Usually particles entrain one another and $D_c > 0$, i.e., the hydrodynamic interaction enhances the collective mode and suppresses the relative one.

To leading order in a/R and a/x , the flow field induced by the motion of one particle in the vicinity of the other is that of a point force. This fluid velocity per unit force is the change in the mobility of the entrained particle. Thus $D_c(x) \simeq k_B T G(x)$, where G is the xx component of the Stokes-flow Oseen tensor (Green's function) in a channel. Using the diffusivity in an unbounded fluid, $D_0 = k_B T / (6\pi\mu a)$ (μ being the fluid viscosity), we define two rescaled coupling diffusivities,

$$\Delta^\pm(\xi) \equiv \frac{D^\pm(\xi) - D_s}{(a/R)D_0}, \quad \xi \equiv x/R, \quad (2)$$

which are experimentally measurable and, within our far-field approximation, *parameter-free* (apart from the unknown geometrical factor γ).

We now substitute the known solution for the Oseen tensor at the center of a cylindrical tube [14, 15] to obtain

$$\begin{aligned} \Delta^\pm(\xi) &= \pm(3/4) \sum_{n=1}^{\infty} [a_n \cos(\beta_n \xi) + b_n \sin(\beta_n \xi)] e^{-\alpha_n \xi} \\ &\simeq \begin{cases} \pm 3/(2\xi), & \xi \ll 1 \\ \pm(3/4)[a_1 \cos(\beta_1 \xi) + b_1 \sin(\beta_1 \xi)] e^{-\alpha_1 \xi}, & \xi \gg 1 \end{cases} \quad (3) \end{aligned}$$

In Eq. (3) $u_n = \alpha_n + i\beta_n$ are the complex roots of the equation $u[J_0^2(u) + J_1^2(u)] = 2J_0(u)J_1(u)$, and $(a_n + ib_n) = 2\{\pi[2J_1(u_n)Y_0(u_n) - u_n(J_0(u_n)Y_0(u_n) + J_1(u_n)Y_1(u_n))] - u_n\} / J_1^2(u_n)$ [J_k and Y_k being the Bessel functions of the first and second (Neumann) kind]. The coupling as a function of distance is depicted in Fig. 3. For $\xi \ll 1$ the particles are insensitive to the walls and the coupling approaches the algebraic $\sim 1/\xi$ dependence as in an unbounded fluid [11]. Yet, for $\xi > 1$ the confined geometry becomes manifest; the sum is dominated by its first term and the interaction decays exponentially with distance. (The coefficients of this term are $a_1 \simeq -0.0370$, $b_1 \simeq 13.8$, $\alpha_1 \simeq 4.47$, and $\beta_1 \simeq 1.47$.)

The sharp screening beyond the confinement length is unique to the linear geometry and is caused by the boundary conditions at the channel walls. We may visualize the boundary conditions as replaced by an infinite

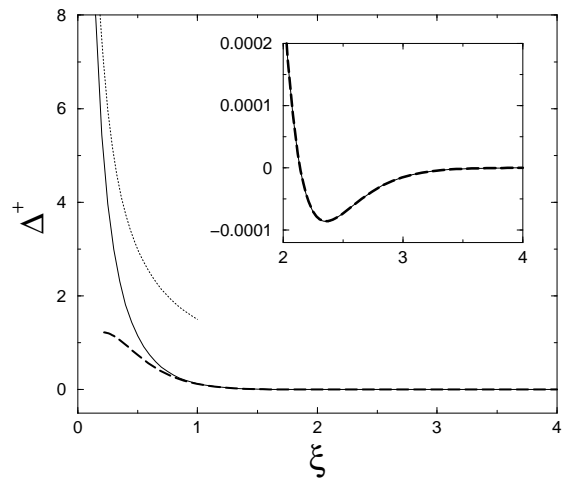


FIG. 3: Rescaled coupling diffusivity Δ^+ ($= -\Delta^-$) as a function of rescaled inter-particle distance $\xi = x/R$ [Eq. (3), solid curve]. At very small distances the curve approaches the algebraic $\sim 1/\xi$ dependence as in an unbounded fluid (dotted line). At large distances it decays exponentially (dashed line). For $\xi \gtrsim 2.14$ the coupling becomes negative (inset).

series of image forces transverse to the channel axis, accompanying the moving particle [12]. At distances larger than the channel width the images cancel the effect of the actual force. Small oscillations on top of the exponential decay make the coupling change sign at $\xi \simeq 2.14$ (Fig. 3, inset). This is a very peculiar effect, implying that for large distances the particles inhibit each other's motion rather than aid it. Physically, this arises from flow rolls that form along the channel [15]. Unfortunately, as seen in Fig. 3, even if the effect still exists in our partially open channel, it is far too small to be currently detectable [19].

In Fig. 4 we have replotted the experimental data of Fig. 2, scaled according to Eq. (2), with $\gamma = 2.44$ for the square cross-section (samples 1 and 2) and $\gamma = 2.72$ for the rectangular one (sample 3). The data for different channel widths, sphere sizes, and densities collapse onto two universal curves for the collective and relative diffusivities. The collapse confirms that the observed coupling is well described by a two-body hydrodynamic interaction within a first-order approximation in a/w . Moreover, considering our crude approximations, the agreement between the universal curve and Eq. (3) is remarkable. The stokeslet approximation thus provides a surprisingly reasonable description of the hydrodynamic interaction even for relatively large particles and short inter-particle distances. We can further use the fitted γ to calculate the expected self-diffusivity which, at the same level of approximation [11], is given by $D_s \simeq D_0(1 - 2.10444a/R)$, $R = \gamma w/2$. This yields for samples 1, 2 and 3 $D_s \simeq 0.16, 0.045$ and $0.040 \mu\text{m}^2/\text{s}$, respectively. Although these values are not far off the measured (low-density) ones— $0.11, 0.036$ and $0.028 \mu\text{m}^2/\text{s}$ —

the differences, compared to the good agreement in Fig. 4, indicate that the self-diffusivity is more sensitive than the two-particle coupling to higher orders in a/w [20].

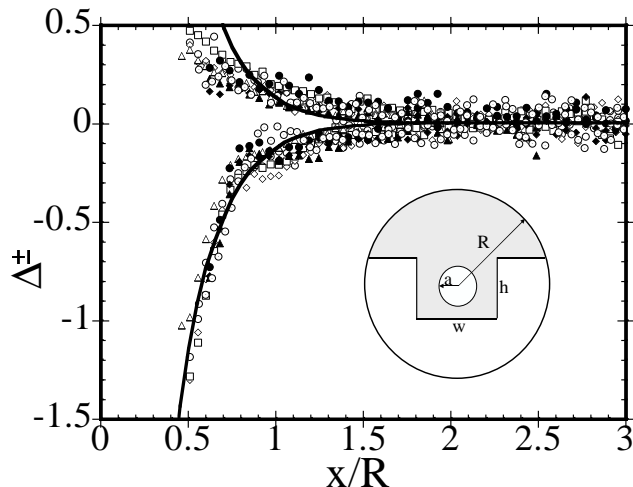


FIG. 4: Rescaled coupling diffusivities Δ^\pm as a function of rescaled inter-particle distance $\xi = x/R$ for all the data of Fig. 2. The solid line is the theoretical curve for a particle in a cylindrical tube (Fig. 3). The inset shows a cross-section of the sample cell with its theoretical effective cylinder.

A small but systematic discrepancy between the calculation and experiment is seen in Fig. 4 as the distance becomes very small. This deviation naturally marks the breakdown of the $x \gg a$ assumption. The observed trend can be understood by considering the extreme case of two particles in contact. The relative diffusivity then vanishes, hence $\Delta^- \rightarrow -D_s/(D_0 a/R)$, whereas the collective one becomes equal to twice the self-diffusivity of a rigid “train” of two touching particles, $2D_2$. Since, evidently, $D_2 < D_s$, we have $\Delta^+ \rightarrow (2D_2 - D_s)/(D_0 a/R) < |\Delta^-|$, in accord with the observed asymmetry.

Another important consequence of the screened coupling is that concerted motion of neighboring particles becomes appreciable at a sharply defined density, comparable to $1/R$; this dynamic clustering will be studied in more detail in a future publication. Our results suggest that a tube-stokeslet approximation [i.e., Eq. (3)] should give a good estimate of the hydrodynamic interaction in *any* linear geometry, provided that the particles are repelled from the walls and one has an estimate for the geometrical factor γ . Although we have discussed only freely diffusing particles, since mobilities are proportional to diffusivities, the same conclusions apply to driven motion as well [21], and should also bear upon motion and patterning in microfluidic systems [22].

We thank Stuart Rice for generous laboratory support, and David Andelman, Cristian Huepe, Leo Kadanoff, Detlef Lohse, Tom Witten, and Wendy Zhang for helpful comments. The experimental work was supported by the National Science Foundation [DMR-9870437 (POWRE)

and CHE-9977841] and the NSF MRSEC program at the University of Chicago (DMR-9808595). HD was also supported by the NSF (DMR-9975533 and DMR-0094569), and the David and Lucile Packard Foundation (99-1465).

* Electronic address: b-lin@uchicago.edu

- [1] J. Kärger and D. M. Ruthven, *Diffusion in Zeolites and Other Microporous Solids* (Wiley, New York, 1992).
- [2] D. J. Aidley and P. R. Stanfield, *Ion Channels: Molecules in Action* (Cambridge University Press, New York, 1996).
- [3] D. G. Levitt, Phys. Rev. A **8**, 3050 (1973). S. Alexander and P. Pincus, Phys. Rev. B **18**, 2011 (1978). J. Kärger, Phys. Rev. A **45**, 4173 (1992). J. Kärger, Phys. Rev. E **47**, 1427 (1993). K. Hahn and J. Kärger, J. Phys. A Math. Gen. **28**, 3061 (1995). Q.-H. Wei, C. Bechinger and P. Leiderer, Science **287**, 625 (2000).
- [4] B. Lin, B. Cui, J.-H. Lee and J. Yu, Europhys. Lett. **57**, 724 (2002).
- [5] P. N. Segrè, E. Herbolzheimer and P. M. Chaikin, Phys. Rev. Lett. **79**, 2574 (1997). M. P. Brenner, Phys. Fluids **11**, 754 (1999).
- [6] B. Lin, J. Yu and S. A. Rice, Phys. Rev. E **62**, 3909 (2000).
- [7] E. R. Dufresne, T. M. Squires, M. P. Brenner and D. G. Grier, Phys. Rev. Lett. **85**, 3317 (2000).
- [8] T. M. Squires and M. P. Brenner, Phys. Rev. Lett. **85**, 4976 (2000).
- [9] E. R. Dufresne, D. Altman and D. G. Grier, Europhys. Lett. **53**, 264 (2001).
- [10] T. M. Squires, J. Fluid Mech. **443**, 403 (2001).
- [11] J. Happel and H. Brenner, *Low Reynolds Number Hydrodynamics* (Martinus Nijhoff, Dordrecht, 1983).
- [12] C. Pozrikidis, *Boundary Integral and Singularity Methods for Linearized Viscous Flow* (Cambridge University Press, New York, 1992).
- [13] N. Liron and S. Mochon, J. Eng. Math. **10**, 287 (1976).
- [14] N. Liron and S. Shahar, J. Fluid Mech. **86**, 727 (1978).
- [15] J. R. Blake, J. Fluid Mech. **95**, 209 (1979).
- [16] B. Cui, B. Lin, S. Sharma and S. A. Rice, J. Chem. Phys. **116**, 3119 (2002).
- [17] In the way D_s is measured here it corresponds to a particle that has no neighbors on one side but can have nearby particles on its other side. The change in D_s at high density arises from a high probability for a third sphere to be located less than the screening length away.
- [18] Significant boundary slip has been recently demonstrated for confined viscous liquids. Still, according to these measurements, no-slip boundary conditions should be the valid case for our system. V. S. J. Craig, C. Neto and D. R. M. Williams, Phys. Rev. Lett. **87**, 054504 (2001).
- [19] Sign reversal of hydrodynamic interactions under confinement is a real effect. We have recently measured negative transverse couplings in a two-plate geometry (to be reported elsewhere).
- [20] A good estimate for D_s can also be obtained by superposing the effects of the three walls [4].
- [21] G.-H. Zheng, R. L. Powell and P. Stroevé, Chem. Eng. Comm. **117**, 89 (1992).
- [22] T. Thorsen, R. W. Roberts, F. H. Arnold and S. R. Quake, Phys. Rev. Lett. **86**, 4163 (2001).